Engineering Surfaces for Substrate-Mediated Gene Delivery Using Recombinant Proteins

Jennifer C. Rea,[†,⊥] Romie F. Gibly,[†] Nicolynn E. Davis,[‡] Annelise E. Barron,[‡] and Lonnie D. Shea*[,†,§]

Department of Chemical and Biological Engineering, Northwestern University, Evanston, Illinois 60208, Department of Bioengineering, Stanford University, Stanford, California 94305, and Robert H. Lurie Comprehensive Cancer Center, Northwestern University, Chicago, Illinois 60611

Received June 3, 2009; Revised Manuscript Received August 10, 2009

Immobilized fibronectin and other natural proteins have been utilized to enhance substrate-mediated gene delivery, with apparent contributions from the intrinsic bioactivity and also physical properties of the immobilized proteins. In this report, we investigated the use of recombinant proteins, compared to the full-length fibronectin protein, as surface coatings for gene delivery to investigate the mechanisms by which fibronectin enhances gene transfer. The recombinant fibronectin fragment $FNIII_{7-10}$ (FNIII) contains the $\alpha_5\beta_1$ binding domain of fibronectin and supports cell adhesion, whereas the recombinant protein polymer PP-12 is also negatively charged and has a molecular weight similar to FNIII, but lacks cell binding domains. Transfection was compared on surfaces modified with FNIII, full-length fibronectin, or PP-12. The full-length fibronectin provided the greatest extent of transgene expression relative to FNIII or PP-12, which was consistent with the amount of DNA that associated with cells. FNIII had 4.2-fold or 4.7-fold lower expression levels relative to fibronectin for polyplexes and lipoplexes, respectively. PP-12 produced expression levels that were 317-fold and 12.0-fold less than fibronectin for polyplexes and lipoplexes, respectively. Although expression was greater on FNIII relative to PP-12, the levels of DNA associated per cell with FNIII were similar to or less than those with PP-12, suggesting that the bioactive sequences may contribute to an enhanced intracellular trafficking. For lipoplexes delivered on FNIII, the efficiency of intracellular trafficking and levels of caveolar DNA were greater than that observed with either the full-length fibronectin or PP-12. For polyplexes, fibronectin fragment resulted in greater intracellular trafficking efficiency compared to PP-12 protein polymer. Recombinant proteins can be employed in place of full-length extracellular matrix proteins for substrate-mediated gene delivery, and bioactive sequences can influence one or more steps in the gene delivery process to maximize transfection.

Introduction

Biomaterial-based approaches to gene delivery have many therapeutic and research applications such as tissue engineering and functional genomics. Gene transfer from the surface of a biomaterial, termed reverse transfection,[1] solid-phase delivery,[2] or substrate-mediated delivery,[3] immobilizes DNA vectors onto a surface as opposed to more typical bolus delivery from the media. Several approaches have been employed for DNA immobilization including DNA entrapment in gelatin,[1] polyelectrolyte layering of DNA,[4,5] or immobilization of preformed complexes with specific tethering[3,6,7] or nonspecific adsorption.[2,8−13] Immobilization by nonspecific adsorption can reduce the amount of DNA required for expression, increase transgene expression and increase the number of cells expressing the transgene relative to similar quantities delivered as a bolus.[8,13]

Fibronectin enhances substrate-mediated gene delivery with retroviruses and DNA/polymer complexes, termed polyplexes.[14,15] For polyplexes, fibronectin mediated the greatest levels of transgene expression compared to other extracellular matrix (ECM) proteins, such as laminin and collagen.[14] Fibronectin is internalized by a caveolin-dependent pathway,[16] and vectors associated with fibronectin may similarly be internalized via caveolae-mediated endocytosis. Thus, the ECM protein targets the vector toward a specific internalization pathway that can influence the ultimate fate of the vector, as internalization via caveolae-mediated endocytosis may avoid the lysosome and subsequent degradation relative to internalization via clathrin-mediated endocytosis.[17,18] Fibronectin could thus be employed to coat biomaterials to enhance gene transfer from the surface; however, naturally derived proteins may not be ideal for immobilization for biomaterial applications, particularly in vivo, due to their large molecular weights, potential antigenicity, and cost. Recombinant proteins, which have customizable amino acid sequences that may mimic some or all of the functions of the full-length protein, may circumvent these disadvantages as they generally have a reduced antigenicity relative to full-length proteins, and lower cost. In addition, recombinant proteins are advantageous over synthetic peptides, because the short length of peptides likely has substantially reduced bioactivity and specificity compared to the full-length proteins. Taken together, recombinant proteins may be engineered to enhanced gene delivery from biomaterials.

Recombinant fibronectin-mimetic proteins have been created to replicate functional properties of full-length fibronectin, with the recombinant proteins demonstrating properties of the functional motifs encoded in them.[19,20] One fibronectin-mimetic protein, in particular, fibronectin fragment $FNIII_{7-10}$, includes

* To whom correspondence should be addressed. Phone: +1-847-491-7043. Fax: +1-847-491-3728. E-mail: l-shea@northwestern.edu.
† Department of Chemical and Biological Engineering, Northwestern University.
‡ Stanford University.
§ Robert H. Lurie Comprehensive Cancer Center.
⊥ Current address: Genentech, Inc., 1 DNA Way, South San Francisco, CA 94080.

10.1021/bm900628e CCC: $40.75
Published on Web 09/23/2009

the RGD motif on the 10th type III repeat of fibronectin and the proline-histidine-serine-arginine-asparagine (PHSRN) "synergy" domain on the ninth type III repeat.[21] These binding domains synergistically bind to $\alpha_5\beta_1$ integrins to significantly increase adhesion strength compared to each domain alone.[21] The $FNIII_{7-10}$ fibronectin fragment has been used to engineer surfaces that direct integrin $\alpha_5\beta_1$ binding for cell adhesion.[21] These fibronectin-mimetic proteins may also direct endocytosis and subsequent internalization and may be utilized to overcome rate-limiting steps to efficient substrate-mediated gene delivery.

In this report, we investigate the use of recombinant proteins, compared to the full-length fibronectin protein, as surface coatings for gene delivery with polyplexes and lipoplexes to investigate the mechanisms by which the fibronectin enhances gene transfer. Polyplexes and lipoplexes were immobilized to substrates coated with fibronectin, fibronectin fragment, and a negatively charged protein polymer designed to be of similar molecular weight as fibronectin fragment but without cell adhesion sites. Transfected cells were visualized on the surface using fluorescence microscopy and transfection was quantified by luciferase assay. The amount of DNA bound to the surface and associated to cells was measured as a function of protein coating and vector. DNA delivery efficiencies and intracellular trafficking efficiencies were calculated for each condition. Finally, quantitative confocal microscopy was used to determine the amount of exogenous DNA that colocalizes with caveolae, which indicates trafficking down a pathway that may avoid lysosomal degradation. These studies identify the potential of recombinant proteins to replace full-length extracellular matrix proteins for gene delivery from biomaterials and may contribute to the design of engineered biomaterial surfaces for applications such as regenerative medicine.

Materials and Methods

Materials. *E. coli* strain BLR(DE3) and plasmid pET-19b were purchased from Novagen (Madison, WI). *E. coli* strain Top10, plasmid pUC18, SYTO 82 nucleic acid fluorescent dye, Alexa Fluor 488 cholera toxin B and Lipofectamine (LF) transfection reagent were purchased from Invitrogen (Carlsbad, CA). Plasmids encoding for β-galactosidase (pβGal) and luciferase/enhanced green fluorescent fusion protein (pEGFP-Luc) with a CMV promoter were purchased from Clontech (Mountain View, CA) and purified from bacteria culture using Qiagen (Valencia, CA) reagents and stored in Tris-EDTA buffer (10 mM Tris, 1 mM EDTA, pH 7.4). α-^{32}P-dATP was purchased from Perkin Elmer (Waltham, MA). Restriction enzymes were purchased from New England Biolabs (Beverly, MA). Taq polymerase was purchased from Promega (Madison, WI). Synthetic oligonucleotides and primers were supplied by Integrated DNA Technologies (Coralville, IA). Branched polyethyleneimine (25 kDa), ampicillin, and fibronectin were purchased from Sigma-Aldrich (St. Louis, MO). All other reagents were obtained from Fisher Scientific (Waltham, MA) unless otherwise noted.

Gene Design and Synthesis for PP-12. Cloning and molecular biology techniques were performed using standard procedures unless otherwise noted. For PP-12, the DNA sequences encoding the monomers of the protein polymer amino acids were designed to incorporate the codon preferences for *Escherichia coli* and to prevent DNA and RNA secondary structure formation that may inhibit cloning and expression. DNA oligonucleotides encoding the protein polymer PP-12 were amplified by PCR and purified by electrophoresis on a 2% agarose gel and excised with the QIAquick Gel Extraction Kit (Qiagen, Valencia, CA). After *Ear*I digestion and purification, the monomers were self-ligated by T4 ligase to form multimers. The multimers were ligated into the cloning vector pUC18 and transformed into NovaBlue cells (Novagen Inc., Madison, WI). Concatemer genes were created by the controlled cloning method with the restriction enzyme *Ear*I as an analog to *Eam*1104 I.[14] Briefly, the plasmid containing multimers was amplified by PCR primers to eliminate one of the flanking *Sap*I sites. The plasmids were split into two fractions; one was digested by *Ear*I and the other was digested with *Sap*I. The *Ear*I fraction was dephosphorylated with calf intestinal phosphatase and then ligated to the *Sap*I digested fraction. The 5′ terminal phosphate group was replaced on the resulting concatamer using T4 polynucleotide kinase and then the concatemer was digested with *Ear*I. This gene was ligated into pUC18 and transformed into NovaBlue cloning cells. Single colonies were isolated and gene insertion was verified by an *Ear*I digestion and visualized on a 2% agarose gel. This process was repeated to obtain genes of the desired length.

The expression vector, pET-19b, was modified to remove the internal *Sap* I site using QuickChange Site-Directed Mutagenesis (Stratagene, La Jolla, CA) to change a single base in the restriction site. The mutated vector was then amplified by PCR with primers containing *Ear*I recognition sites as well as a stop codon. The amplified linear plasmid was digested with *Ear*I to create complementary termini for the concatemer genes. These genes were ligated into the plasmid with T4 DNA ligase and transformed into NovaBlue cells. Correct insertion was verified by electrophoresis of double digested genes with *Bam*HI and *Nde*I restriction enzymes and through DNA sequencing (SeqWright, Houston, TX). The ligation into the expression vector resulted in the gene of interest expressed as a fusion protein with an *N*-terminal histidine tag (tag amino acid sequence: GH_{10}SSGHIDDDDKHM).

Protein Polymer Expression and Purification. Plasmids containing the desired gene were transformed into *E. coli* expression strain BLR(DE3) cells. A 5 mL starter culture in LB Broth was grown with a single colony for 8 h. The starter culture was used to inoculate an overnight 100 mL LB broth culture, both supplemented with 200 μg/mL ampicillin and 12.5 μg/mL tetracycline. Cultures of Difco Terrific Broth (1 L), supplemented with 200 μg/mL ampicillin and 12.5 μg/mL tetracycline, were inoculated with 15−20 mL from the overnight culture. The culture was induced with 0.5 mM isopropyl thiogalactoside (IPTG; U.S. Biologicals, Swampscott, MA) when the OD_{600} was between 0.6 and 0.8. The cells were harvested after 4 h by centrifugation and the cell pellet was resuspended in 6 M guanidine hydrochloride, 20 mM sodium phosphate, 500 mM NaCl, pH 7.8 buffer. The cells were lysed by three successive freeze/thaw cycles followed by sonication. Cellular debris was removed by centrifugation for 40 min at 6000 *g* at 4 °C. The protein was purified with Chelating Sepharose Fast Flow nickel-charged resin (GE Healthcare, Piscataway, NJ) under denaturing conditions with imidazole competitive elution. The fractions containing purified protein, as determined by sodium dodecyl sulfate polyacrylamide gel electrophoresis (SDS-PAGE), were dialyzed against deionized water and then lyophilized. Molecular weight was verified using MALDI-TOF mass spectrometry.

Expression and Purification of Fibronectin Fragment III_{7-10}. *E. coli* transformed with plasmid for expressing fibronectin fragment III_{7-10} was a kind gift from Harold Erickson at Duke University. A 50 mL starter culture in LB Broth with 100 μg/mL ampicillin was grown with a single colony overnight. The started culture was used to inoculate an 800 mL LB broth culture, supplemented with 100 μg/mL ampicillin. The culture was induced with 0.4 mM isopropyl thiogalactoside (IPTG) when the OD_{600} was between 0.7 and 1.0. The cells were harvested after 4 h by centrifugation, and the cell pellet was resuspended in CelLytic B Cell Lysis reagent (Sigma-Aldrich, St. Louis, MO) at 5 mL lysis buffer per gram of pellet and 5 μg/mL DNase I. The cell suspension was then agitated for 30 min at 4 °C. Cellular debris was removed by centrifugation for 15 min at 10000 *g* at 4 °C. The protein in the supernatant was then precipitated with 40% ammonium sulfate and centrifuged. The protein layer was removed and dissolved in 0.2 M Tris, pH 8.0, and dialyzed to remove ammonium sulfate. The sample was then filtered using a 0.22 μm filter and purified on an anion exchange column using an AKTAprime FPLC (GE Healthcare, Piscataway, NJ) with 1 M NaCl competitive elution. The fractions containing purified protein, as determined by sodium dodecyl sulfate

Table 1. Physical Properties of Protein Coatings

name	description	molecular weight	total charge
PP-12 protein polymer	recombinant protein polymer $[(LQQQGGAGTGSA)_2(GAGQGEA)_3]_{12}$	45905	−39
fibronectin fragment $FNIII_{7-10}$	recombinant protein with PHSRN synergy sequence and RGD adhesion sequence of fibronectin	39946	−14
fibronectin	heterodimeric extracellular matrix protein	440000	−100

polyacrylamide gel electrophoresis (SDS-PAGE), were dialyzed against deionized water and then lyophilized. Molecular weight was verified using MALDI-TOF mass spectrometry.

Substrate Coating, Complex Formation, and Immobilization. Surfaces for DNA immobilization and cell seeding were prepared by adsorption of proteins to tissue-culture polystyrene (TCPS) plates (96-well). Protein coatings were prepared at a concentration of 1 mg/mL in double deionized water (ddH_2O), and 8.33 μL of protein solution was added to wells containing 100 μL of ddH_2O. Wells were allowed to dry completely prior to the addition of DNA complexes.

Polyethyleneimine (PEI) was dissolved in 0.1 M sodium bicarbonate and dialyzed against ddH_2O overnight with a Pierce Snakeskin 10000 MWCO dialysis membrane, lyophilized, and reconstituted in Tris-buffered saline (TBS, pH 7.4) prior to complex formation. PEI/DNA complexes, termed polyplexes, were formed at an N/P (nitrogen/phosphate) ratio of 10 in TBS using 0.42 μg DNA per well. Polyplexes were formed by the addition of PEI to plasmid, resulting in self-assembled colloidal particles. This solution was mixed gently by pipetting, and the mixture was allowed to incubate for 20 min at room temperature. LF, a 3:1 w/w formulation of the polycationic lipid 2,3-dioleyloxy-*N*-[2(sperminecarboxamido)ethyl]-*N*,*N*-dimethyl-1-propanaminium trifluoroacetate (DOSPA) and the neutral lipid dioleoyl phosphatidylethanolamine (DOPE), was used at a 5:1 w/w ratio with DNA. Lipid/DNA complexes, termed lipoplexes, were formed by adding LF solution dropwise to a solution containing DNA, using 0.42 μg DNA per well. This solution was mixed gently by pipetting, and the mixture was allowed to incubate for 20 min at room temperature. Lipoplexes were formed in serum-free cell growth media (Dulbecco's Modified Eagle Medium (DMEM), Invitrogen, Carlsbad, CA) at pH 7.4. Immediately after complex formation, polyplexes and lipoplexes were incubated on the substrates for 2 h by adding 10 μL of complexes to 50 μL of TBS for polyplexes and 50 μL of DMEM for lipoplexes, and were then washed twice in TBS for polyplexes and DMEM for lipoplexes to remove unbound complexes.

Cell Culture and Transfection. Transfection studies were performed with NIH/3T3 mouse fibroblasts (ATCC, Manassas, VA) cultured at 37 °C and 5% CO_2 in DMEM supplemented with 1% sodium pyruvate, 1% penicillin-streptomycin, 1.5 g/L $NaHCO_3$, and 10% fetal bovine serum (cDMEM). Cells were seeded at a density of 5000 cells per well in 96-well plates (100 μL total volume) and added immediately after complex immobilization. Transfection results were obtained 24 h post-transfection by measuring the extent of transgene expression. The extent of transgene expression was quantified by measuring the luciferase activity using the Luciferase Assay System (Promega, Madison, WI). The luminometer was set for a 3 s delay with signal integration for 10 s. Luciferase activity was normalized to the amount of total protein in the sample, which was measured using a BCA assay (Pierce, Rockford, IL) following the manufacturer's instructions. All studies were carried out in triplicate. To visualize EGFP in transfected cells, NIH/3T3 cells were transfected with pEGFP-Luc as described above and visualized using a Leica epifluorescent microscope (Bannockburn, IL) fitted with a FITC filter and equipped with a digital camera.

Quantification of DNA Bound to the Substrate. The amount of DNA bound to the surface after complex immobilization was determined using plasmids radiolabeled with α-^{32}P dATP. A nick translation kit (Amersham Pharmacia Biotech, Piscataway, NJ) was used to radiolabel pβGal following the manufacturer's protocol with minor modifications. Complexes were formed as described above with radiolabeled DNA and immobilized onto a 96-well plate with detachable wells. Immobilized complexes were washed twice to remove unbound complexes, and the amount of DNA bound to the surface was determined by immersing samples in 5 mL of Biosafe II scintillation cocktail (Research Products International Corp., Mount Prospect, IL) for measurement with a scintillation counter. The counts were correlated to DNA concentration using a standard curve.

Quantification of Cell-Associated DNA. Complexes were formed with radiolabeled DNA as described above and immobilized onto a 96-well plate. Immobilized complexes were washed twice to remove unbound complexes, and cells were seeded as described above. After incubation at 37 °C and 5% CO_2 for 24 h, cells were harvested by washing twice with 1× PBS (phosphate-buffered saline), adding 50 μL of trypsin-EDTA for 2 min to detach the cells, then adding 150 μL of cDMEM to quench the trypsin. Cells were further dislodged from the surface by scraping. Cells were centrifuged for 5 min at 5000 *g* and resuspended in 200 μL of 1× PBS. The amount of DNA bound to the cells was determined by immersing samples in 5 mL of scintillation cocktail for measurement with a scintillation counter. The counts were correlated to DNA concentration using a standard curve. The measurement of cell-associated DNA includes complexed and uncomplexed DNA. The efficiency of DNA delivery was calculated as the percentage of surface-bound DNA that is cell-associated. The efficiency of intracellular trafficking was calculated as protein expressed, that is, relative light units per mg of total protein per well (RLU/mg protein) per ng of DNA associated to cells.

Imaging and Quantification of Plasmid in Caveolae. Plasmids encoding for β-galactosidase were labeled with Cy5 using a Label IT nucleic acid labeling kit (Mirus) according to the manufacturer's instructions. Briefly, DNA and Label IT reagents were mixed and incubated at 37 °C for 1 h. After incubation, DNA was precipitated with ethanol and resuspended in 10 μL of Tris-EDTA (TE) buffer. NIH/3T3 cells were transfected in 8-well glass chamber slides (Nalge Nunc International, Rochester, NY), as described above. An inverted Leica LCS DM-IRE2 confocal microscope was used to image live cells, which were imaged through a 40× oil-immersion objective with a field of view of 375 × 375 mm, with *Z*-sections taken every 366.3 nm. The resulting image resolution was 2048 × 2048 pixels, and *Z*-sections were taken to image the entirety of cells within the *X*,*Y* field of view, producing a voxel size of 183 × 183 × 366 nm (*X*,*Y*,*Z*). Cy5-labeled plasmid was excited by a 10 mW HeNe laser at 633 nm and fluorescence was observed at 645−725 nm. Nuclear compartments were visualized by incubating cells with 0.2 μL Syto 82 nucleic acid stain for 5 min at room temperature prior to excitation by a 1 mW GreNe laser at 543 nm and fluorescence was observed at 555−600 nm. Lipid rafts/caveolae were visualized as described previously with minor modifications,[22,23] with cells incubated with 20 μL of Alexa Flour 488 cholera toxin B for 20 min at room temperature prior to excitation by an Ar laser at 488 nm, and fluorescence was observed at 495−515 nm. Sequential scanning was used to control for spectral overlap between fluorophores, with 4× line averaging to improve signal-to-noise ratios.

Quantification of DNA complex localization within subcellular compartments was performed using NIH ImageJ (http://rsb.info.nih.gov/ij/). Several plug-ins were used to facilitate colocalization. Adaptive-3DThreshold, a part of the MBF "ImageJ for Microscopy" Collection (www.macbiophotonics.ca/imagej/) was used to identify cytoplasmic and nuclear compartments based on the differential intensity of Syto 82 staining of cytoplasmic mRNA and nuclear DNA. The Object Counter3D plug-in (http://rsb.info.nih.gov/ij/ plugins/track/objects.html)

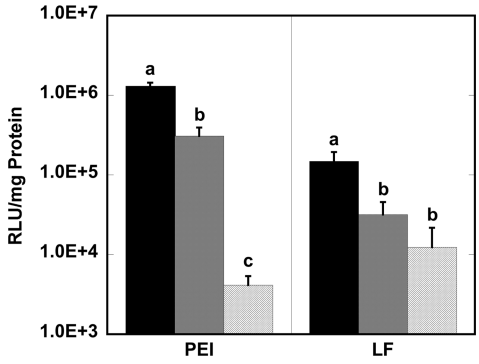

Figure 1. Transfection of NIH/3T3 cells on protein-coated substrates. Luciferase expression by NIH/3T3 cells cultured on polystyrene with adsorbed fibronectin (black bars), fibronectin fragment $FNIII_{7-10}$ (gray bars), and protein polymer (hashed bars) is shown as a function of delivery vector (PEI = polyethyleneimine, LF = Lipofectamine). Luciferase levels are reported as relative light units (RLU) normalized by total cellular protein in the sample well. Data is presented as an average of triplicate measurements ± standard deviation of the mean. A statistically significant difference ($p < 0.05$) is denoted with different letters within the same vector condition.

was used to define cellular compartments based upon their volumes, allowing multiple cells to be simultaneously identified and characterized. ColocalizationHighlighter, also part of the MBF Collection, was used to colocalize DNA complexes to caveolar compartments. Colocalized voxels were counted and compared to total cellular DNA for each condition. An average of 43 cells were captured per image stack, and at least three image stacks were analyzed per condition.

Statistics. Statistical analysis was performed using JMP software (SAS Institute, Inc., Cary, NC). Comparative analyses were completed using one-way ANOVA with Tukey post-tests, at a 95% confidence level. Mean values with standard deviation are reported and all experiments were performed in triplicate with replicates.

Results

Transfection on Immobilized Fibronectin and Recombinant Proteins. Fibronectin, fibronectin fragment $FNIII_{7-10}$ (FNIII), and protein polymer (PP-12) were selected for the studies based on a combination of biological activity and physical properties. The physical properties of the proteins in this study are listed in Table 1. Fibronectin, FNIII, and PP-12 are negatively charged, with FNIII and PP-12 having molecular weights that are approximately one-tenth of the full-length fibronectin heterodimer. FNIII contains the RGD adhesion sequence of fibronectin and the PHSRN synergy sequence, while PP-12 does not contain any known bioactive sequences.

Initial studies investigated transfection on the three proteins. Fibronectin, FNIII, and PP-12 were immobilized to tissue-culture polystyrene prior to the addition of DNA complexes for substrate-mediated gene delivery. A dose response study was performed with immobilized proteins ranging from 0 to 16.67 μg protein dried per well, and the greatest transfection was achieved with 8.33 μg protein for both polyplexes and lipoplexes on fibronectin and FNIII and for lipoplexes on PP-12 (data not shown). Thus, 8.33 μg of protein were immobilized to the substrate for the remainder of this study. For transfection with polyplexes and lipoplexes, fibronectin resulted in the greatest amount of protein expression, which was 4.2-fold and 317-fold greater than the FNIII and PP-12 proteins, respectively, for polyplexes and 4.7-fold and 12.0-fold greater for lipoplexes than the FNIII and PP-12 proteins, respectively (Figure 1). For polyplexes, FNIII had greater transfection compared to PP-12, while for lipoplexes, FNIII had comparable transfection to PP-12. Immobilized FNIII resulted in protein expression levels of up to 3.0×10^5 RLU/mg for polyplexes and 3.1×10^4 RLU/mg for lipoplexes, with a 74-fold increase in protein expression for FNIII compared to PP-12 for polyplexes.

Phase and fluorescence microscopy images depict cells and transfection by polyplexes (Figure 2) and lipoplexes (Figure 3) immobilized to PP-12, FNIII, and fibronectin. An increase in the number of transfected cells was observed for polyplexes for fibronectin-coated surfaces relative to the protein polymer surfaces, and the increase in luciferase levels is consistent with this observation. Phase microscopy images indicate that cell density and morphology are consistent among all surface coatings and vectors used, suggesting comparable cell viability for all conditions.

DNA Binding to the Surface. The quantity of DNA immobilized to the coated surfaces was subsequently investigated. For polyplexes, increased DNA immobilization was observed with FNIII compared to fibronectin and PP-12, with fibronectin and PP-12 having comparable amounts of DNA on the substrate (Figure 4). In contrast, fibronectin yielded the greatest amount of DNA binding for lipoplexes, with PP-12 yielding greater amounts of DNA on the surface compared to FNIII. Thus, the amount of DNA bound to protein-coated surfaces is dependent on both the identity of the protein coating as well as the vector. The greatest quantities of DNA on fibronectin-coated surfaces are consistent with the greatest levels of expression on fibronectin for lipoplexes. However, the transfection results between FNIII and PP-12 do not follow the trends associated with the quantities of DNA. Thus, we subsequently quantified the association of DNA to cells for each protein coating and vector to investigate the efficiency of DNA delivery from the surfaces.

DNA Association and Efficiency of Delivery. Fibronectin resulted in the greatest amount of DNA associated to cells for both polyplexes and lipoplexes, with a 1.7-fold and 47-fold increase in DNA association compared to FNIII for polyplexes and lipoplexes, respectively (Figure 5). While FNIII had greater DNA association to cells than PP-12 for polyplexes, DNA association to cells for FNIII was lower than PP-12 for lipoplexes.

The efficiency of DNA delivery, defined as the percentage of surface-bound DNA that is cell-associated, was quantified to investigate the interaction between cells, DNA complexes, and protein coatings. For polyplexes and lipoplexes, fibronectin coating resulted in the greatest DNA delivery efficiency, with 41.3 and 25.0% of surface-bound DNA reaching the cells for polyplexes and lipoplexes, respectively (Table 2). The full-length protein resulted in the greatest DNA delivery efficiency.

Efficiency of Intracellular Trafficking. The intracellular trafficking efficiency of cell-associated DNA, defined as the efficiency of DNA to traverse the cytoplasm, enter the nucleus and be transcribed to express the desired protein, was next quantified by normalizing transfection to the amount of DNA associated to cells. For polyplexes, fibronectin resulted in the greatest efficiency of intracellular trafficking, followed by FNIII, which was significantly greater than PP-12 (Figure 6). However, for lipoplexes, FNIII had the greatest intracellular trafficking efficiency, with fibronectin and PP-12 efficiencies being comparable.

We subsequently investigated the quantity of DNA in caveolae as a percentage of cellular DNA, as previous studies have indicated that fibronectin internalization occurs by a caveolin-dependent pathway, and gene delivery from immobilized fibronectin had greater internalization through caveolae.[14] Caveolae can be considered as a specialized form of

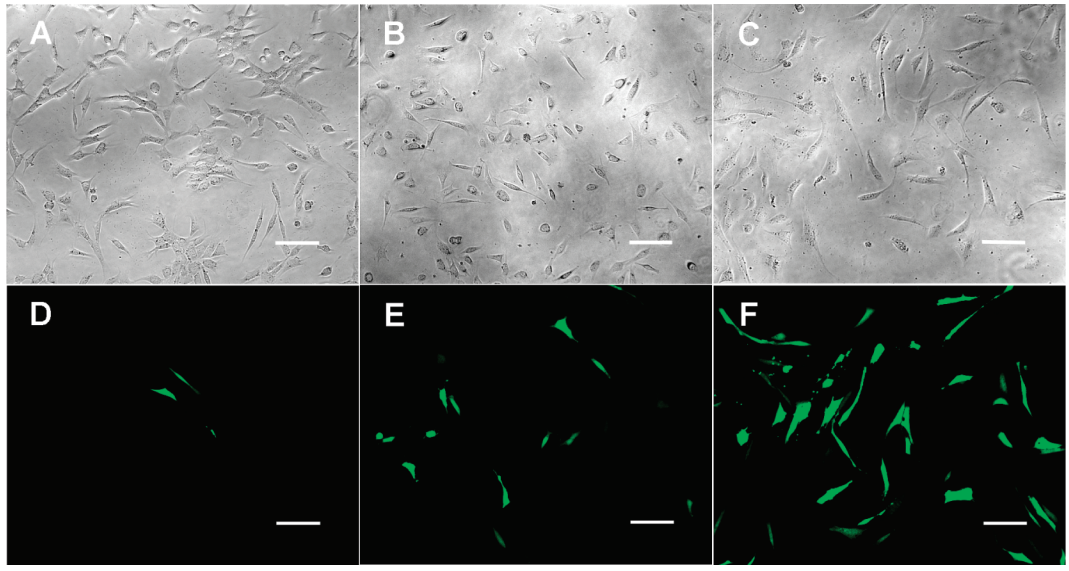

Figure 2. Phase and fluorescence microscopy images of transfected cells. Representative images of NIH/3T3 cells transfected with PEI/DNA complexes immobilized to protein polymer (A,D), fibronectin fragment (B,E), and fibronectin (C,F) are shown. Images were captured with a 20× objective. Cells expressing enhanced green fluorescent protein (EGFP) are shown in green. Scale bar indicates 25 μm.

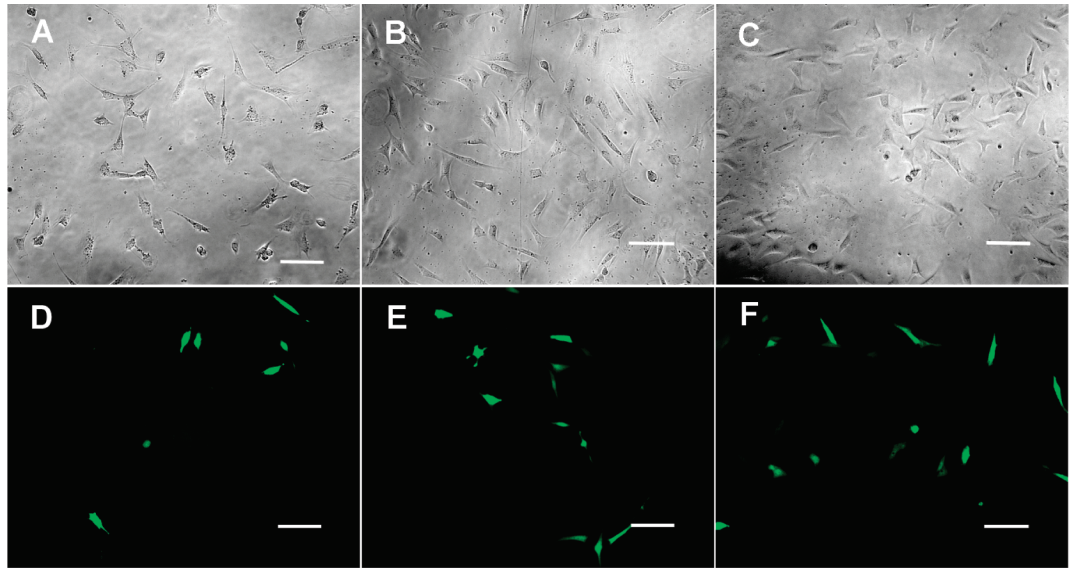

Figure 3. Phase microscopy and fluorescence microscopy images of transfected cells. Representative images of NIH/3T3 cells transfected with Lipofectamine/DNA complexes immobilized to protein polymer (A,D), fibronectin fragment (B,E), and fibronectin (C,F) are shown. Images were captured with a 20× objective. Cells expressing enhanced green fluorescent protein (EGFP) are shown in green. Scale bar indicates 25 μm.

lipid rafts, and particles taken up by the caveolae-mediated pathway are delivered to caveosomes, which are pre-existing, stable organelles with a neutral pH.[24,25] Internalization via caveolae-mediated endocytosis is hypothesized to avoid the lysosome and subsequent degradation relative to internalization via clathrin-mediated endocytosis, which may enhance gene transfer.[26] Cholera toxin B (CTB) is known to be a selective marker for the caveolae/raft mediated pathway.[25] Thus, Alexa Fluor 488 CTB and Cy5-labeled DNA were used to determine the extent of colocalization of DNA within caveosomes. For lipoplexes, FNIII resulted in the greatest percentage of caveolar DNA, with 58.0% of cellular DNA being colocalized to caveolae (Figure 7). Fibronectin and PP-12 had comparable amounts of caveolar DNA for lipoplexes. Interestingly, for polyplexes, the amount of caveolar DNA did not significantly differ among protein coatings.

Discussion

In this report, we investigated the use of recombinant proteins as surface coatings for gene delivery with polyplexes and lipoplexes to investigate the mechanisms by which fibronectin enhances gene transfer. The full-length fibronectin provided the greatest extent of transgene expression, which was 4.2-fold and 317-fold greater than the FNIII and PP-12 proteins, respectively, for polyplexes, and 4.7-fold and 12.0-fold greater for lipoplexes than the FNIII and PP-12 proteins, respectively. Although fibronectin resulted in the greatest protein expression and DNA association per cell for both polyplexes and lipoplexes, recombinant fibronectin fragment resulted in greater efficiency of intracellular trafficking, and greater caveolar DNA for lipoplexes compared to full-length fibronectin and protein polymer without bioactive sequences. These results suggest that the bioactivity of the fibronectin fragment contributes to enhanced transfection

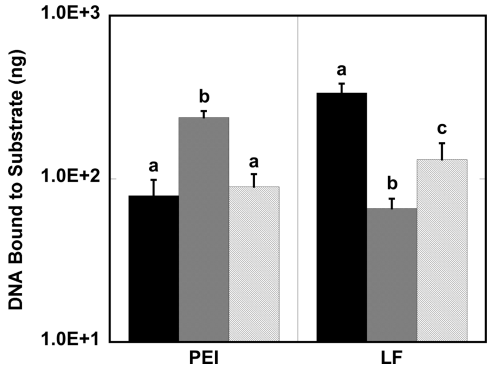

Figure 4. DNA immobilization to the substrate. The amount of DNA immobilized to polystyrene with adsorbed fibronectin (black bars), fibronectin fragment $FNIII_{7-10}$ (gray bars), and protein polymer (hashed bars) was measured as a function of delivery vector. Data is presented as an average of triplicate measurements ± standard deviation of the mean. A statistically significant difference ($p < 0.05$) is denoted with different letters within the same vector condition.

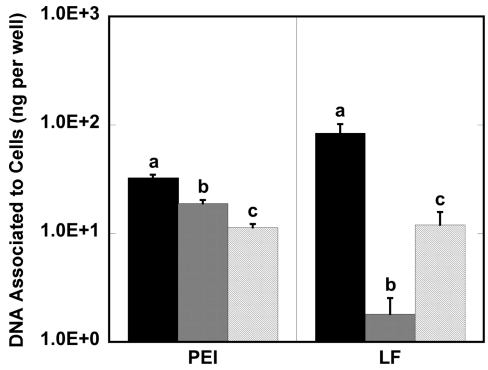

Figure 5. Plasmid association to cells. NIH/3T3 cells were transfected by surface delivery from polystyrene coated with fibronectin (black bars), fibronectin fragment $FNIII_{7-10}$ (gray bars), and protein polymer (hashed bars). The number of plasmid copies associated per cell is shown as a function of delivery vector. Data is presented as an average of triplicate measurements ± standard deviation of the mean. A statistically significant difference ($p < 0.05$) is denoted with different letters within the same vector condition.

Table 2. Efficiency of DNA Delivery from the Substrate to the Cells[a]

	PEI	LF
FN	41.3 ± 2.7	25.0 ± 5.1
FNIII	7.9 ± 0.6	2.8 ± 1.1
PP-12	12.7 ± 1.0	9.2 ± 2.8

[a] NIH/3T3 cells were transfected by surface delivery of DNA complexes from protein-coated polystyrene. The amount of cell-associated DNA, as a percentage of substrate-bound DNA, is reported as a function of the vector.

and intracellular trafficking compared to the protein polymer without bioactive sequences for lipoplexes.

Substrate-mediated transfection with lipoplexes has been limited by cell-association.[26] Thus, because fibronectin delivered the most DNA to the cells, the greatest transfection was achieved despite lower intracellular trafficking efficiency compared to FNIII for lipoplexes. This increased cellular association of DNA was consistent with an increased DNA binding to the surface and increased efficiency of DNA delivery from the substrate. The length of fibronectin may contribute to its enhanced binding of lipoplexes relative to recombinant proteins. Fibronectin has a molecular weight that is an order of magnitude greater than either FNIII or PP-12. This increased length of fibronectin relative to the recombinant proteins may increase available

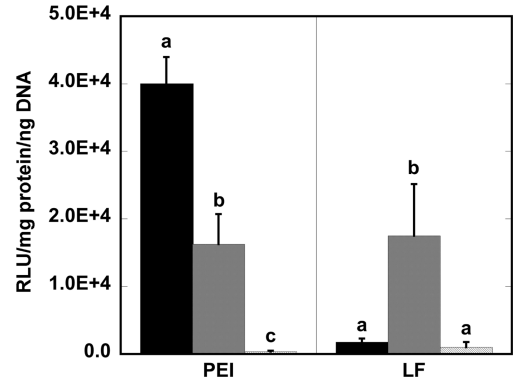

Figure 6. Efficiency of intracellular trafficking. NIH/3T3 cells were transfected by surface delivery from polystyrene coated with fibronectin (black bars), fibronectin fragment $FNIII_{7-10}$ (gray bars), and protein polymer (hashed bars). Luciferase expression is normalized by the amount of cell-associated DNA and presented as a function of protein coating and vector. Data is presented as an average of triplicate measurements ± standard deviation of the mean. A statistically significant difference ($p < 0.05$) is denoted with different letters within the same vector condition.

binding sites for lipoplexes, and thereby increase nonspecific binding of lipoplexes (unpublished observations). Alternatively, other regions of fibronectin outside of FNIII may either facilitate binding or serve to maintain the activity of the lipoplexes by preventing structural changes.[27] The potential exists to incorporate additional groups into the FNIII protein polymer using recombinant techniques,[28] which could increase the length and potentially provide additional function groups to mediate lipoplex binding.

The conformation of adsorbed proteins on the surface may affect the biological activity and its subsequent interaction with DNA complexes and cells. Previous reports have demonstrated that adsorption of fibronectin to different surfaces alters protein structure and modulates integrin binding, cell adhesion, cell spreading, and cell migration.[29−31] In this report, fibronectin was adsorbed to tissue culture polystyrene (TCPS), which had previously been shown to increase transfection substantially compared to uncoated TCPS and other extracellular matrix proteins.[14] For fibronectin, protein unfolding due to the availability of immobilization sites on the surface increases the availability of cell-binding domains and can thus promote complex internalization. With FNIII, the cell-binding domains may be readily available without the need for protein unfolding due to the short length of the fragment relative to full-length fibronectin. An important consideration is that the physical properties of the substrate may also be designed to impact adsorbed protein conformation and complex potency, which has the potential to increase DNA delivery to cells and enhance transfection.[27]

The fibronectin fragment $FNIII_{7-10}$ promoted the most efficient intracellular trafficking of lipopexes, with the greatest quantities of caveolar DNA for FNIII compared to fibronectin and PP-12. The bioactivity of fibronectin fragment $FNIII_{7-10}$ influences endocytosis and subsequent intracellular trafficking, possibly due to its interaction with integrins. The same mass of each protein was immobilized, thus, there was a greater number of RGD adhesion sites for FNIII surfaces compared to fibronectin due to the lower molecular weight of FNIII. This increased number of cell binding sites for FNIII could contribute to the observed increase in caveolar DNA compared to fibronectin for lipoplexes. The binding sites alone can support and promote cell adhesion and migration, as RGD peptides and fragments

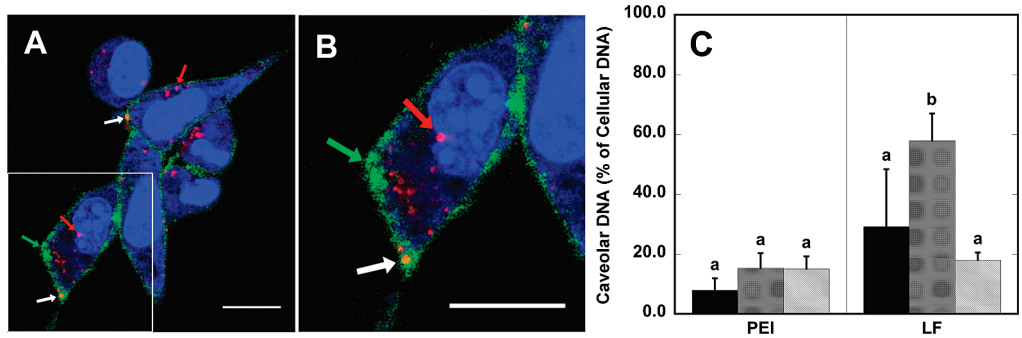

Figure 7. Colocalization of Cy5-labeled plasmid with caveolae within NIH/3T3 cells was quantified using confocal microscopy. Blue indicates nuclear and cytoplasmic nucleic acids, red indicates Cy5-labeled plasmid, and green indicates caveolae (A). Red arrows indicate Cy5-labeled DNA, green arrows indicate caveolae, and white arrows indicate colocalized Cy5-labeled DNA and caveolae. Magnified section of A is presented, as indicated by outline (B). Scale bars indicate 15 μm. Confocal images above depict transfected cells with Lipofectamine on PP-12 protein polymer. NIH/3T3 cells were transfected by surface delivery from polystyrene coated with fibronectin (black bars), fibronectin fragment $FNIII_{7-10}$ (gray bars), and protein polymer (hashed bars), and caveolar DNA was calculated as a percentage of cellular DNA (C). Data is presented as an average of triplicate measurements $\pm$ standard deviation of the mean. A statistically significant difference ($p < 0.05$) is denoted with different letters within the same vector condition.

of fibronectin that contain the RGD cell binding site promoted clustering of the $\alpha5\beta1$ integrin in focal adhesions; however, clustering of fibronectin-binding integrins alone may not be sufficient to trigger increased cell growth.[32] Thus, although fibronectin fragment demonstrated the most efficient intracellular trafficking of lipoplexes, it may lack other bioactive properties of fibronectin that can positively affect cellular processes such as cell growth.

Polyplexes delivered from a surface have been limited by their potency,[26] yet the results herein suggest that the potency of polyplexes is retained with fibronectin, allowing for increased efficiency of delivery and increased efficiency of intracellular trafficking despite lower amounts of DNA bound to the surface compared to FNIII. Although the quantities of DNA may be low, the delivery efficiency is relatively high for fibronectin, which may result from the surface promoting an native conformation of the polyplex or a targeted delivery to specific pathways.[26,27] Interestingly, FNIII resulted in increased transfection and efficiency of intracellular trafficking compared to PP-12, suggesting that the cell adhesion sequences in FNIII play an active role in transfection. The delivery of polyplexes from the FNIII coated substrate may target the polyplexes toward pathways that lead to efficient delivery to the nucleus. Although an increase in caveolar DNA is not observed for polyplexes delivered from an FNIII-coated surface, other intracellular processes such as the trafficking of endosomes along the actin cytoskeleton, the escape of DNA from the endosome, or nuclear entry may be affected for cells cultured on FNIII.

In addition to bioactivity and molecular weight of the proteins, the charge of the recombinant protein coatings may also be engineered for enhanced DNA delivery from a substrate. On self-assembled monolayers (SAMs), the greatest amount of binding and transfection for PEI complexes was observed on surfaces presenting charged, hydrophilic groups, specifically carboxylic acid-terminated thiols.[9] However, in this study, negatively charged protein polymer had the lowest gene expression of all conditions investigated. Compared to self-assembled monolayers, protein coatings assume 3-D architecture on a surface,[33−37] and other amino acid residues, for example, hydrophobic residues, may also play a role in complex binding to the surface. Interestingly, FNIII coating resulted in greater transfection and greater efficiency of intracellular trafficking than the more negatively charged PP-12 for polyplexes, which may indicate a greater role of the bioactive sequences in FNIII in substrate-mediated gene delivery with polyplexes compared to protein charge.

Internalization of viruses, small molecules, and DNA complexes through caveolae-mediated endocytosis may avoid lysosomes, which could increase gene expression.[17,18,22,38] Caveolae were studied in particular because previous results suggest that fibronectin increases transgene expression by directing DNA complex uptake to caveolae.[14] However, fibronectin was not found to increase internalization via caveolae for polyplexes. A previous study suggested that fibronectin targets caveolae for internalization of polyplexes, in which the polyplexes had smaller average diameters and different N/P ratio than those used herein.[14] Endocytic internalization is impacted by particle size,[38] and the larger particles used herein may not become endocytosed through caveolae. Importantly, the approach to evaluate caveolae differed; previously, genistein, which inhibits caveolae-mediated endocytosis, was added to investigate internalization mechanisms.[14,17] However, genistein is a nonspecific tyrosine kinase inhibitor and may decrease transfection through mechanisms other than reducing internalization through caveolae. In this study, confocal microscopy was utilized to directly colocalize DNA with caveolae and lipid rafts. This approach, as opposed to using endocytic inhibitors, more directly connects DNA internalization and caveolae.

Conclusion

This report describes the engineering of protein-coated substrates for substrate-mediated gene delivery, and compares transfection and intracellular trafficking of polyplexes and lipoplexes delivered from recombinant protein surfaces and full-length fibronectin. Surface proteins can influence extracellular events such as vector immobilization and cellular internalization, but may also influence intracellular events such as trafficking. Although full-length fibronectin resulted in the greatest transfection, recombinant fibronectin fragment achieved protein expression levels that were substantial, and increased the efficiency of intracellular trafficking. These results support the potential to design substrates that will promote cellular association and support efficient intracellular trafficking that avoids degradation during intracellular processing. The results herein suggest different mechanisms of transfection on recombinant protein-coated surfaces for polyplexes and lipoplexes and illustrate the potential of recombinant protein-coated surfaces for nonviral gene delivery from biomaterials.

Acknowledgment. Support for this research was provided in part by the NIH (R01 EB003806-01 (AEB, LDS)), the Institute for BioNanotechnology in Medicine (IBNAM) at Northwestern University, and a Ford Foundation Predoctoral Fellowship (J.C.R.). MALDI-TOF mass spectrometry was performed at the Analytical Services Laboratory at Northwestern University. We thank Sheng Ding, Xiao Xiao Wang, Anne Kelly, Alyssa Huang, and Missy Ducommun for technical assistance.

References and Notes

(1) Ziauddin, J.; Sabatini, D. M. *Nature* **2001**, *411* (6833), 107–10.
(2) Bielinska, A. U.; Yen, A.; Wu, H. L.; Zahos, K. M.; Sun, R.; Weiner, N. D.; Baker, J. R., Jr.; Roessler, B. J. *Biomaterials* **2000**, *21* (9), 877–87.
(3) Segura, T.; Volk, M. J.; Shea, L. D. *J. Controlled Release* **2003**, *93* (1), 69–84.
(4) Jewell, C. M.; Zhang, J.; Fredin, N. J.; Lynn, D. M. *J. Controlled Release* **2005**, *106* (1−2), 214–23.
(5) Jewell, C. M.; Zhang, J.; Fredin, N. J.; Wolff, M. R.; Hacker, T. A.; Lynn, D. M. *Biomacromolecules* **2006**, *7* (9), 2483–91.
(6) Segura, T.; Chung, P. H.; Shea, L. D. *Biomaterials* **2005**, *26* (13), 1575–84.
(7) Segura, T.; Shea, L. D. *Bioconjugate Chem.* **2002**, *13* (3), 621–9.
(8) Bengali, Z.; Pannier, A. K.; Segura, T.; Anderson, B. C.; Jang, J. H.; Mustoe, T. A.; Shea, L. D. *Biotechnol. Bioeng.* **2005**, *90* (3), 290–302.
(9) Pannier, A. K.; Anderson, B. C.; Shea, L. D. *Acta Biomater.* **2005**, *1* (5), 511–522.
(10) Shen, H.; Tan, J.; Saltzman, W. M. *Nat. Mater.* **2004**, *3* (8), 569–574.
(11) Yoshikawa, T.; Uchimura, E.; Kishi, M.; Funeriu, D. P.; Miyake, M.; Miyake, J. *J. Controlled Release* **2004**, *96* (2), 227–32.
(12) Jang, J. H.; Rives, C. B.; Shea, L. D. *Mol. Ther.* **2005**, *12* (3), 475–483.
(13) Jang, J. H.; Bengali, Z.; Houchin, T. L.; Shea, L. D. *J. Biomed. Mater. Res.* **2006**, *77A* (1), 50–58.
(14) Bengali, Z.; Rea, J. C.; Shea, L. D. *J. Gene Med.* **2007**, *9* (8), 668–678.
(15) Gersbach, C. A.; Coyer, S. R.; Le Doux, J. M.; Garcia, A. J. *Biomaterials* **2007**, *28* (34), 5121–5127.
(16) Sottile, J.; Chandler, J. *Mol. Biol. Cell* **2005**, *16* (2), 757–768.
(17) Rejman, J.; Bragonzi, A.; Conese, M. *Mol. Ther.* **2005**, *12* (3), 468–474.
(18) Bathori, G.; Cervenak, L.; Karadi, I. *Crit. Rev. Ther. Drug Carrier Syst.* **2004**, *21* (2), 67–95.
(19) Kurihara, H.; Morita, T.; Shinkai, M.; Nagamune, T. *Biotechnol. Lett.* **2005**, *27* (9), 665–670.
(20) Kurihara, H.; Nagamune, T. *J. Biosci. Bioeng.* **2005**, *100* (1), 82–87.
(21) Cutler, S. M.; Garcia, A. J. *Biomaterials* **2003**, *24* (10), 1759–1770.
(22) Pelkmans, L.; Helenius, A. *Traffic* **2002**, *3* (5), 311–320.
(23) van der Aa, M. A. E. M.; Huth, U. S.; Hafele, S. Y.; Schubert, R.; Oosting, R. S.; Mastrobattista, E.; Hennink, W. E.; Peschka-Suss, R.; Koning, G. A.; Crommelin, D. J. A. *Pharm. Res.* **2007**, *24* (8), 1590–1598.
(24) Orlandi, P. a.; Fishman, P. H. *J. Cell Biol.* **1998**, *141* (4), 905–915.
(25) Tiruppathi, C.; Naqvi, T.; Wu, Y. B.; Vogel, S. M.; Minshall, R. D.; Malik, A. B. *Proc. Natl. Acad. Sci. U.S.A.* **2004**, *101* (20), 7699–7704.
(26) Bengali, Z.; Rea, J. C.; Gibly, R. F.; Shea, L. D. *Biotechnol. Bioeng.* **2009**, *102* (6), 1679–1691.
(27) Pannier, a. K.; Wieland, J. A.; Shea, L. D. *Acta Biomater.* **2008**, *4* (1), 26–39.
(28) Won, J. I.; Barron, A. E. *Macromolecules* **2002**, *35* (22), 8281–8287.
(29) Michael, K. E.; Vernekar, V. N.; Keselowsky, B. G.; Meredith, J. C.; Latour, R. A.; Garcia, A. J. *Langmuir* **2003**, *19* (19), 8033–8040.
(30) Garcia, A. J.; Vega, M. D.; Boettiger, D. *Mol. Biol. Cell* **1999**, *10* (3), 785–798.
(31) Keselowsky, B. G.; Collard, D. M.; Garcia, A. J. *J. Biomed. Mater. Res.* **2003**, *66A* (2), 247–259.
(32) Sottile, J.; Hocking, D. C.; Swiatek, P. J. *J. Cell Sci.* **1998**, *111*, 2933–2943.
(33) Akiyama, S. K.; Aota, S.; Yamada, K. M. *Cell Adhes. Commun.* **1995**, *3* (1), 13–25.
(34) Lewandowska, K.; Balachander, N.; Sukenik, C. N.; Culp, L. a. *J. Cell. Physiol.* **1989**, *141* (2), 334–345.
(35) Kowalczynska, H. M.; Nowak-Wyrzykowska, M.; Kolos, R.; Dobkowski, J.; Kaminski, J. *J. Biomed. Mater. Res.* **2005**, *72A* (2), 228–236.
(36) Koenig, A. L.; Gambillara, V.; Grainger, D. W. *J. Biomed. Mater. Res.* **2003**, *64A* (1), 20–37.
(37) Pierschbacher, M.; Hayman, E. G.; Ruoslahti, E. *Proc. Natl. Acad. Sci. U.S.A.* **1983**, *80* (5), 1224–1227.
(38) Rejman, J.; Oberle, V.; Zuhorn, I. S.; Hoekstra, D. *Biochem. J.* **2004**, *377*, 159–169.

BM900628E